EVALUATION OF NUMERICAL SCHEMES TO SOLVE SHOCK WAVE DISCONTINUITIES

Edmar Alino da Cruz Silva, edmaralino@gmail.com
Instituto Tecnológico de Aeronáutica, CTA/ITA, São José dos Campos, SP, 12228-900, Brazil
João Luiz F. Azevedo, joaoluiz.azevedo@gmail.com
Instituto de Aeronáutica e Espaço, CTA/IAE, São José dos Campos, SP, 12228-903, Brazil

Abstract. *The main objective of the present research work consists of studying flux schemes to solve shock wave discontinuities. Several schemes are considered, mostly based on Godunov-type methods which use approximate solutions of a local Riemman problem. Flux-vector splitting and centered schemes are also used. A 1-D shock tube problem is considered as the testbed for this study. Results from Roe, HLLC, centered, van Leer, and AUSM schemes are compared to theoretical Riemman problem solutions, such as Sod's shock-tube problem. These schemes are implemented in a 1-D finite volume framework. Time integration is performed with an explicit, 4th-order Runge-Kutta scheme. High-order spatial discretization is achieved with a 5-point-stencil MUSCL interpolation scheme. Limiter functions are incorporated to obtain non-oscillatory resolution of discontinuities and steep gradients, without smearing. The quality of the results are evaluated based on the presence, or absence, of oscillatory solutions, shock wave smearing, and acoustic and entropy wave speeds.*
Keywords: *Riemann Problem, Flux Limiters, Godunov-type Methods, MUSCL, Shock Wave.*

1. INTRODUCTION

Discontinuities, such as shock waves, lead to computational difficulties and the intent of this work is to evaluate the accuracy of methods that approximate such solutions. Classical discretization methods can be expected to break down near discontinuities. The work concentrates primarily on high resolution finite volume methods that have gained recognition for being very effective for computing discontinuous solutions. The goal, for these methods, is to capture discontinuities in the solutions automatically, without explicitly tracking them. Discontinuities are, then, spread over one or more grid cells. Sucess requires that the methods implicitly incorporate the correct jump conditions, reduce smearing to a minimum, and do not introduce non-physical oscillations near the discontinuities. The methods evaluated in the present work are: central differencing, van Leer flux splitting, advection upstream splitting, Roe flux differencing splitting and Harten-Lax-van Leer contact discontinuity difference splitting schemes.
The Riemann problem test cases represent a shock tube experiment under three different initial conditions. A shock tube is just a metal tube in which the gas at low pressure and the gas at high pressure are separated using a diaphragm. This diaphragm suddenly bursts open under predetermined conditions to produce a shock wave that travels down the low pressure section of the tube. Simultaneously, a rarefaction wave, often referred to as an expansion fan, travels back into the driver gas. The section that represents the interface separating the driven and driver gases is called the contact surface. The contact surface moves rapidly along the tube behind the shock front. The first two test cases are Sod problems [Sod, 1978]. Test case 1 is a shock-tube with moderate initial pressure ratio while test case 2 has higher initial pressure ratio. The last test case is a severe compression shock tube, characterized by a membrane bursting causing two identical gases to move towards each other at Mach 25 [Batten, 1997]. All three test cases have exact solutions.

2. FINITE VOLUME METHOD

The theoretical background upon which the numerical code is based is discussed herein. The Euler equations, which describe the fluid motion under the hypothesis of continuum, are briefly discussed herein. The equations are derived from the physical balance of fluxes in a given fluid cell, considering the conservation of mass and energy, and Newton's 2nd law, within the control volume and restricted to 1D flows. For detailed discussion and derivation refer to [Leveque, 2002]. The Euler equations governing the flow of a compressible gas in 1D comprise

$$\begin{aligned} &\frac{\partial \rho}{\partial t} + \frac{\partial}{\partial x}(\rho u) = 0 \\ &\frac{\partial}{\partial t}(\rho u) + \frac{\partial}{\partial x}(\rho u u + p) = 0 \\ &\frac{\partial}{\partial t}(E) + \frac{\partial}{\partial x}[(E + p)u] = 0 \end{aligned} \tag{1}$$

where ρ is the density, t is the time, x is the position, u_i is the fluid velocity, p is the pressure and E is the total energy per unit mass of fluid. The equations first term is the transient term and the second terms are the flux term derivative.

$$E = \frac{p}{\gamma - 1} + \frac{1}{2}\rho|u|^2 \tag{2}$$

where γ is the ratio of specific heats. The above equations are closed by taking an equation of state, the simplest being the ideal gas

$$p = \rho RT, \tag{3}$$

where R is the gas constant and T is the absolute temperature.

3. FLUX SCHEMES

Flux calculation algorithms are supposed to accurately evaluate the flux quantities at the left and right cell face boundaries. A flux calculation algorithm must be of such a form that it calculates the flux at given cell boundary based on cell values only to the upstream side of the boundary for supersonic flow, and from both sides of the boundary for subsonic flows. This procedure is further complicated by the fact that a schock wave will create a situation where supersonic flow is present on one side of the shock and subsonic flow on the other side. Several early flux discretizations schemes were shown to poorly handle discontinuities, such as shock waves. Nowadays, there are a large number of techniques available which perform this task. For the purposes here, five of the schemes were selected to be tested. These five schemes were selected simply because of their popularity, their recognizability by most users, and their body of testing and documentation.
The Euler equations are a system of homogeneous conservation laws,

$$q_t + F(q)_x = 0, \tag{4}$$

where $F(q)_x$ is the flux-function and q is the properties vector.

3.1 CENTRAL DIFFERENCING SCHEME

One of the methods to compute the numerical flux is the Central Differencing Scheme (CDS), which calculates the cell-face value as an average between the adjacent cells. This scheme is 2nd-order accurate and requires the explicit addition of artificial dissipation terms in order to control nonlinear instabilities that will arise in the flow simulation. In the present formulation, the Mavripilis scalar switched model is used to compute the dissipation. The centered spatial discretization of the convective fluxes in this scheme is as presented in Jameson, Turkish and Schmid [Jameson et al., 1981]. The convective operator is the sum of the inviscid fluxes on the i-th volume faces and the artificial dissipation operator is built by a blend of undivided Laplacian and bi-harmonic operators. In regions of high property gradients, the bi-harmonic operator is turned off in order to avoid oscillations. In smooth regions, the undivided Laplacian operator is turned off in order to mantain 2nd order accuracy. A numerical pressure sensor is responsible for this switching between the operators. In the multistage Runge-Kutta time integration the artificial dissipation operator is calculated on all stages. The expressions for the flux, convection and dissipation operators are given by

$$\begin{aligned}
&F_i = C_i - D_i, \\
&C_i = \sum_{k=1}^{2} P(q_k) S_k, \quad q_k = \frac{1}{2}(q_i + q_m), \quad P(q) = \left\{ \begin{array}{c} \rho u \\ \rho u^2 + p \\ (e+p)u \end{array} \right\}, \\
&D_i = \sum_{k=1}^{2} \left\{ \frac{1}{2}(A_i + A_m)[\epsilon_2(Q_m - Q_i) - \epsilon_4(\nabla^2 q_m - \nabla^2 q_i)] \right\},
\end{aligned} \tag{5}$$

where F_i, C_i and D_i are respectively flux, convection and dissipation operators in cell i. m represents the adjacent cells. P is the production operator, S is the face area, q_k, q_i and q_m are respectively the properties in the cell and adjacent cells. A_i and A_m are matrix coefficients; ρ, u, p and e stand for density, speed, pressure and energy. A numerical pressure sensor, ν_i, is responsible for the switching between the operators. In this work, K_2 and K_4 are constants assumed equal 1/4 and

3/256, respectively [Bigarella, 2007].

$$\epsilon_2 = K_2 max(\nu_i, \nu_m), \quad \epsilon_4 = max(0, K_4 - \epsilon_2), \quad \nu_i = \frac{\sum_{m=1}^{2} \|p_m - p_i\|}{\sum_{m=1}^{2} \|p_m + p_i\|} \tag{6}$$

3.2 FLUX VECTOR SPLITTING UPWIND SCHEMES

3.2.1 VAN LEER FLUX SPLITTING

The van Leer flux vector splitting scheme [van Leer, 1982] is analyzed to determine its eigenvalues, which are the wave speeds of the equation set for the Euler equations. For the quasi 1-D equation set, there are three speeds: [u+a, u, and u-a]. The flux is split into the respective contributions from each wave speed, with a "positive" or "left" flux component coming from the positve wave speeds and a "negative" or "right" flux component coming from the negative wave speeds. If the flow is supersonic, only the flux component from the upstream direction is non-zero. For subsonic flow, both the left and right flux components are non-zero. The van Leer flux components are defined as given in eqn. (7), which results from the Mach number splitting. Van Leer put these components in terms of Mach number, M, to make the analysis more consistent.

$$F^{\pm} = \left\{ \begin{array}{l} [\pm\frac{1}{4}\rho a(M \pm 1)^2] \\ \\ [\pm\frac{1}{4}\rho a(M \pm 1)^2][(\gamma - 1)Ma \pm 2a]\frac{1}{\gamma} \\ \\ [\pm\frac{1}{4}\rho a(M \pm 1)^2][(\gamma - 1)Ma \pm 2a]\frac{1}{2(\gamma^2 - 1)} \end{array} \right\} \tag{7}$$

where $\pm$ represents right and left adjacent cells properties, respectively. a is sound speed and γ denotes the ratio of specific heat capacity of the gas. The van Leer method is sometimes criticized for being "too dissipative," and it was even recommended by van Leer himself only for use in the Euler equations. As pointed out by van Leer [van Leer, 1982], the van Leer flux splitting scheme fails to recognize the contact discontinuity, leading to excessive numerical diffusion. Hence significant error appears in the viscous region which can not be simply cured by reducing size and using higher-order differencing [Liou et al., 1993].

3.2.2 ADVECTION UPSTREAM SPLITTING SCHEME

According to [Liou et al., 1993], the Advection Upstream Splitting Scheme (AUSM) is a tentative approach to combine the efficiency of flux-vector splitting (FVS) and the accuracy of flux-difference splitting (FDS) methods. This scheme has the intent of being simple and accurate, yielding vanishing numerical diffusivity at the stagnation points. In a variety of Euler calculations performed, the accuracy of the present scheme is shown to be rivaling that of Roe's splitting. Since the scheme has no matrix operation is much simpler to construct, and thus, more efficient. Furthermore, unlike Roe's scheme [Roe, 1981], this method does not involve differentiation of fluxes, hence it is smoother. This is desirable for the general equation of state where a stiff variation of thermodynamic states may occur in certain transitional states. The flux at any cell boundary is defined by eqn. (8).

$$F = (M_L^+ + M_R^-) \left\{ \begin{array}{c} \rho a \\ \rho u a \\ \rho a h_0 \end{array} \right\}_{(L or R)} + \left\{ \begin{array}{c} 0 \\ P_L^+ + P_R^- \\ 0 \end{array} \right\} \tag{8}$$

where $M^{\pm}$ and $P^{\pm}$ are defined in eqn. (6) and (7) and ρ is density, a is sound speed and h is enthalpy. L and R stand for left and right.

$$M^{\pm} = \left\{ \begin{array}{ll} \pm\frac{1}{4}(M \pm 1)^2 & if \quad |M| \leq 1 \\ \\ \frac{1}{2}(M \pm |M|) & if \quad |M| > 1 \end{array} \right. \tag{9}$$

$$P^{\pm} = \begin{cases} \pm\dfrac{P}{4}(M \pm 1)^2(2 \mp M) & if \quad |M| \leq 1 \\ \dfrac{P}{2}\dfrac{(M \pm |M|)}{M} & if \quad |M| > 1 \end{cases} \tag{10}$$

where M is Mach number and P is pressure. Meanwhile, AUSM flux vector splitting method has many similarities with van Leer method. However, in AUSM, the pressure term of the flux is split apart from the convective part of the flux. The convective part of the flux is calculated using either a left or right biased stencil depending on the sign of an averaged, convective Mach number. The pressure component of the flux is split similarly to the Van Leer concept into a left running and a right running pressure flux.

3.3 FLUX DIFFERENCE SPLITTING SCHEMES

3.3.1 ROE FLUX DIFFERENCE SPLITTING WITH ENTROPY CORRECTION

In Roe scheme [Roe, 1981], the flux calculation is treated as a series of 1-D Riemann problems. For each eigenvalue/wave speed, a Riemann problem is solved. For the Euler equations, this Riemann problem is non-linear, and the effort to solve is large. Although the early solution to this non-linear series of problems was a significant step forward for the CFD community, Roe proposed to solve an "approximate" linear version of the Riemann problem. This resulted in much faster execution and very little accuracy is sacrificed in the process. In addition, the Roe scheme automatically admits shocks as a possible solution without any extra effort.

$$F = \frac{1}{2}\left(A(q)[q_R - q_L]\right) - \frac{1}{2}\sum_{k=1}^{3}\left(e_{RL,i} * \phi(\lambda_i) * \Delta w_i\right) \tag{11}$$

where $A(q)$, e_{RL}, Δw_i and $\phi(\lambda(i)$ are defined by eqn (9), (10), (11) and (12). F is the flux.

$$A(q) = \begin{bmatrix} 0 & 1 & 0 \\ \dfrac{(\gamma-3)}{2}u^2 & (3-\gamma)u & \gamma - 1 \\ \dfrac{1}{2}(\gamma-1)u^3 - uh_0 & h_0 - (\gamma-1)u^2 & \gamma u \end{bmatrix}, \tag{12}$$

$$e_{RL,1} = \begin{bmatrix} 1 \\ u_{RL} \\ \dfrac{1}{2}u_{RL}^2 \end{bmatrix}, \quad e_{RL,2} = \frac{\rho_{RL}}{2a_{RL}}\begin{bmatrix} 1 \\ u_{RL} + a_{RL} \\ h_{0,RL} + u_{RL}a_{RL} \end{bmatrix}, \quad e_{RL,3} = -\frac{\rho_{RL}}{2a_{RL}}\begin{bmatrix} 1 \\ u_{RL} - a_{RL} \\ h_{0,RL} - u_{RL}a_{RL} \end{bmatrix}, \tag{13}$$

$$\begin{aligned} \Delta w_1 &= \Delta\rho - \frac{\Delta P}{a_{RL}^2}, \\ \Delta w_2 &= \Delta u + \frac{\Delta P}{\rho a_{RL}}, \\ \Delta w_3 &= \Delta u - \frac{\Delta P}{\rho a_{RL}}, \end{aligned} \tag{14}$$

Roe scheme is still one of the most used methods in solving convective equation sets. One major issue with the traditional Roe scheme is that it admits expansion shocks as well as compression shocks. In reality, an expansion shock is not a valid solution of the Euler equations, so the Roe scheme is often supplemented with an "entropy" correction which filters out the possibility of expansion shocks by modifying the eigenvectors that cause the phenomenon. Harten was an early advocate of the entropy correction, and the present work has a basic version of his correction method. [Harten, Lax and van Leer, 1983]

$$\phi(\lambda_i) = \begin{cases} \dfrac{\lambda_i^2 + \delta^2}{2\delta} & for \quad |\lambda_i| < \delta \\ \|\lambda_i| & for \quad |\lambda_i| \geq \delta \end{cases} \tag{15}$$

This equation defines the eigenvalues term in the flux calculation. This correction has the effect of smoothing out expansion shocks, which occur near sonic points because one of the eigenvalues goes to zero at these points. In eqn. (15), δ is a small positive number. As discussed by [Laney, 1998], the choosing of this parameter is somewhat arbitrary and for the present work it is just the velocity jump from right to left.

3.3.2 HARTEN-LAX-VAN LEER CONTACT DISCONTINUITY DIFFERENCE SPLITTING

The Harten-Lax-van Leer contact discontinuity difference splitting scheme (HLLC) is an improved two-state version of the original single-state HLL Riemann solver by Harten, Lax and van Leer [Toro, 1999]. The original HLL numerical flux automatically satisfies entropy inequality [Davis, 1988], resolves isolated shocks [Harten, Lax and van Leer, 1983] and preserves positivity . Batten et al. have shown that the HLLC flux not only preserves the advantageous features of the HLL flux, but also resolves isolated contact discontinuities exactly [Batten, 1997]. The implementation of the HLLC Riemann solver is relatively simple and the computational cost is lower compared with many other available Riemann solvers [Aliabadia, 2005].

$$F_{HLLC} = \begin{cases} F_l & if \quad S_L > 0 \\ F(U_l^*) & if \quad S_L \leq 0 < S_M \\ F(U_r^*) & if \quad S_M \leq 0 < S_R \\ F_r & if \quad S_R < 0 \end{cases}, \tag{16}$$

where

$$F(U_L^*) = \begin{bmatrix} \rho_l^* S_M \\ (\rho_l u)^* S_M + p^* \\ (e_l^* + p^*) S_M, \end{bmatrix}, \qquad F(U_R^*) = \begin{bmatrix} \rho_r^* S_M \\ (\rho_r u)^* S_M + p^* \\ (e_r^* + p^*) S_M \end{bmatrix}, \tag{17}$$

$$P^* = \rho_l (q_l - S_L)(q_L - S_M) + p_L = \rho_r (q_r - S_R)(q_L - S_M) + p_R, \tag{18}$$

and the signal velocities: S_M, S_L and S_R are taken as:

$$\begin{aligned} S_M &= \frac{\rho_r q_r (S_R - q_r) - \rho_l q_l (S_L - q_l) + p_l - p_r}{\rho_r (S_R - q_r) - \rho_l (S_L - q_l)}, \\ S_L &= min[\lambda_1(U_l), \lambda_1(U^{Roe}], \\ S_R &= max[\lambda_m(U^{Roe}), \lambda_m(U_r)]. \end{aligned} \tag{19}$$

with $\lambda_1(U^{Roe})$ and $\lambda_m(U^{Roe})$ being the smallest and largest eigenvalues of the Roe matrix [Roe, 1981].

4. HIGH ORDER RECONSTRUCTION

4.1 GENERAL COMMENTS

High-resolution schemes are used in the numerical solution of partial differential equations where high accuracy is required in the presence of shocks or discontinuities. They have the following properties:

- Second or higher order spatial accuracy is obtained in smooth parts of the solution.
- Solutions are free from spurious oscillations or wiggles.
- High accuracy is obtained around shocks and discontinuities.
- The number of mesh points containing the wave is small compared with a first-order scheme with similar accuracy.

High-resolution schemes often use flux limiters to limit the gradient around shocks or discontinuities. A particularly successful high-resolution scheme is the MUSCL scheme which uses state extrapolation and limiters for better accuracy.

4.2 MUSCL INTERPOLATION

The flux vector splitting and flux difference schemes require that the solution is known at the cell faces in order to evaluate the flux. However, in a finite volume context, properties are only known in the cell centroid. Therefore, properties in the cell face must be somehow computed from the cell centroid and other additional information. It is possible to calculate the flux at the cell centroid and extrapolate it to the boundary, but limited research has indicated that this method is less desirable than calculating the flux at the interface boundaries by extrapolating the solution variables to the same cell faces. So, with this need in mind, the solution available at the cell centres must make use of some kind of geometric extrapolation to estimate the solution at the interface boundaries [MacLean 2008].
For the present work, one established choice has been selected that is known as Monotone Upwind Schemes for Conservation Laws (MUSCL). MUSCL interpolation is actually a brand name for a complete set of reconstruction-evolution methods originally pioneered by Van Leer [van Leer, 1982]. Van Leer constructed the first total variation diminishing (TVD) scheme. It is a finite volume method that provides high accuracy numerical solutions to partial differential equations which can involve solutions that exhibit shocks, discontinuities or large gradients.
The piecewise constant approximation of Godunov's scheme [Godunov, 1959] is replaced by reconstructed states, derived from cell-averaged states obtained from the previous time-step. For each cell, slope limited, reconstructed left and right states are obtained and used to calculate fluxes at the cell boundaries. These fluxes can, in turn, be used as input to a Riemann solver, following which the solutions are averaged and used to advance the solution in time. The reconstruction-evolution technique as programmed is given here:

$$\begin{cases} q_{j+1/2}^{LEFT} & = q_j + \dfrac{\phi}{4} * [(1-k) * (q_j - q_{j-1}) + (1+k) * (q_{j+1} - q_j); \\ q_{j-1/2}^{RIGHT} & = q_j - \dfrac{\phi}{4} * [(1+k) * (q_j - q_{j-1}) + (1-k) * (q_{j+1} - q_j); \end{cases} \tag{20}$$

where $q_{j+1/2}$ and $q_{j-1/2}$ are properties in the right and left faces, respectively. The limiter parameter, ϕ, is a flag for either first order or higher order reconstruction. First order reconstruction can be performed by setting $\phi = 0$. Setting $\phi = 1$ results in higher order reconstruction, which is a useful feature of this method. The valid range for κ is between -1 and 1, inclusive. A value of less than one results in an upwind biased scheme, while a value of exactly one results in a centered scheme. Any value of κ results in a second order reconstruction with the exception of $1/3$, which results in a unique $3rd$ order accurate reconstruction.

4.3 LIMITERS

Flux limiters are the standard way to avoid non-physical oscillations that would otherwise occur with high order spatial discretization schemes due to discontinuities such as shocks. Limiters restrict the forward and backward gradient terms of the MUSCL reconstruction to force the scheme to have the TVD property in a region of strong shocks.
The function $\phi(r_i)$, defined in eqn. (20), is a limiter function that restricts the slope of the piecewise approximations to ensure the solution is TVD, thereby avoiding the spurious oscillations that would otherwise occur around discontinuities or shocks. The accuracy of a TVD discretization degrades to first order at local extrema, but tends to second order over smooth parts of the domain. r represents the ratio of successive gradients on the solution mesh and is given by

$$r_i = \frac{u_i - u_{i-1}}{u_{i+1} - u_i}, \tag{21}$$

where u is the flow speed.

Figure 1 presents the limiters tested in test case 2. The figure is splitted between the limiters results acceptability. The limiters that achieved acceptable results presents lower ϕ and thus a stricter slope control.

5. RESULTS AND DISCUSSION

The shock tube problem constitutes a particularly interesting test case, since it has an exact solution for the full system of one-dimensional Euler equations containing simultaneously a shock wave, a contact discontinuity and an expansion fan. This particular problem, also called Riemann problem, is altogether of practical and theoretical interest. It can be realized experimentally by the sudden breakdown of a diaphragm in a long one-dimensional tube separating two initial gas states at different pressures and densities.

Viscous effects are neglected along the tube walls and a long tube is considered to avoid reflections at the tube ends. Thus, the results can easily be compared with the exact solution. At the bursting of the diaphragm, at time $t = 0$, the

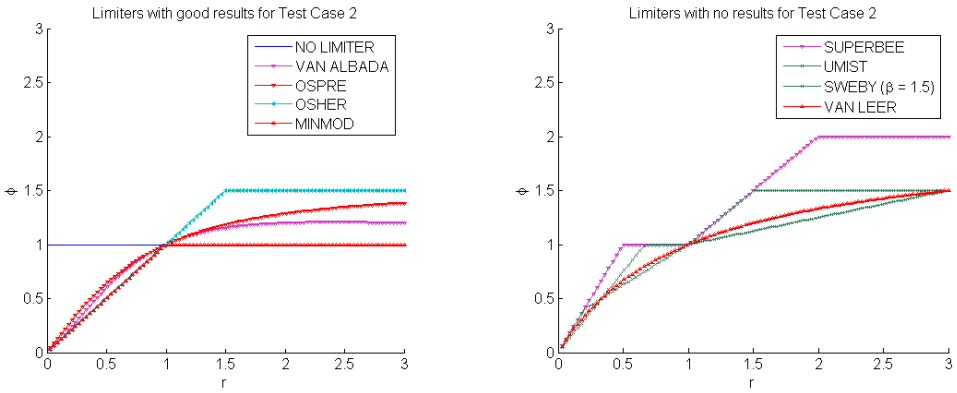

Figure 1. Flux Limiters function ϕ.

pressure discontinuity propagates to the right in the low-pressure gas and, simultaneously, an expansion fan propagates to the left in the high-pressure gas. In addition, a contact discontinuity separating the two gas regions propagates to the right in the tube [Hirsch, 1990].

The proposed schemes are evaluated and compared with the test case exact solutions. Test cases correspond to test data applied by Sod (1978). The Sod problem is an essentially one-dimensional flow discontinuity problem which provides a good test for the compressible scheme ability to capture shocks and contact discontinuities, and to produce the correct density profile in a rarefaction wave. It also tests a scheme ability to correctly satisfy the Rankine-Hugoniot shock jump conditions.

5.1 TEST CASE 1

Test case 1 corresponds to a Sod problem with initial pressure ratio of 10. The results obtained with the proposed schemes are compared to the exact solution in Fig. 2. The following initial conditions, in SI units, were considered for a perfect gas with $\gamma = 1.4$, and the results are taken at $t = 2.2ms$:

$$p_L = 10^5; \quad rho_L = 1; \quad p_R = 10^4; \quad rho_R = 0.125; \quad u_L = u_R = 0$$

The shock pressure ratio is moderate and the density plot is presented in Fig. 2. At $t = 2.2$ ms, three different nonlinear waves are present: an expansion fan between $x = 2.25$ and $x = 4.8$, a contact discontinuity at $x = 7.1$, and a shock at $x = 9.0$. The two sharp discontinuities are resolved satisfactorily, *i.e.*, negligible smearing and acoustic speed differences, with the proposed flux vector splitting schemes and the flux difference splitting schemes. However, the central differencing scheme presented non-physical oscillatory solutions around discontinuities.

5.2 TEST CASE 2

Test case 1 corresponds to a Sod problem with initial pressure ratio of 100. The results obtained with the proposed schemes are compared to the exact solution in Fig. 3. The following initial conditions, in SI units, were considered for a perfect gas with $\gamma = 1.4$, and the results are taken at $t = 2.2ms$:

$$p_L = 10^5; \quad rho_L = 1; \quad p_R = 10^3; \quad rho_R = 0.010; \quad u_L = u_R = 0$$

The shock pressure ratio is severe and the density plot is presented in Fig. 3. At $t = 2.2$ ms, three different nonlinear waves are present: an expansion fan between $x = 4.1$ and $x = 5.8$, a contact discontinuity at $x = 6.3$, and a shock at $x = 7.0$. The methods resolved satisfactorily the expansion fan and the acoustic speed, however presented significant smearing in the discontinuities. Altogether, the central differencing scheme presented non-physical oscillatory solutions around discontinuities. Van Albada flux scheme is used in the upwind schemes.
Figure 4 shows the solutions of test case 2, considering various limiters. The flux limiters are evaluated using HLLC flux scheme. The result with first order reconstruction presents spurious oscillations and smearing throughout the entropy and acoustic waves. Within the flux limiter solutions, Osher presented greater oscillations near the acoustic wave. The remaining methods presented smearing in the acoustic wave.

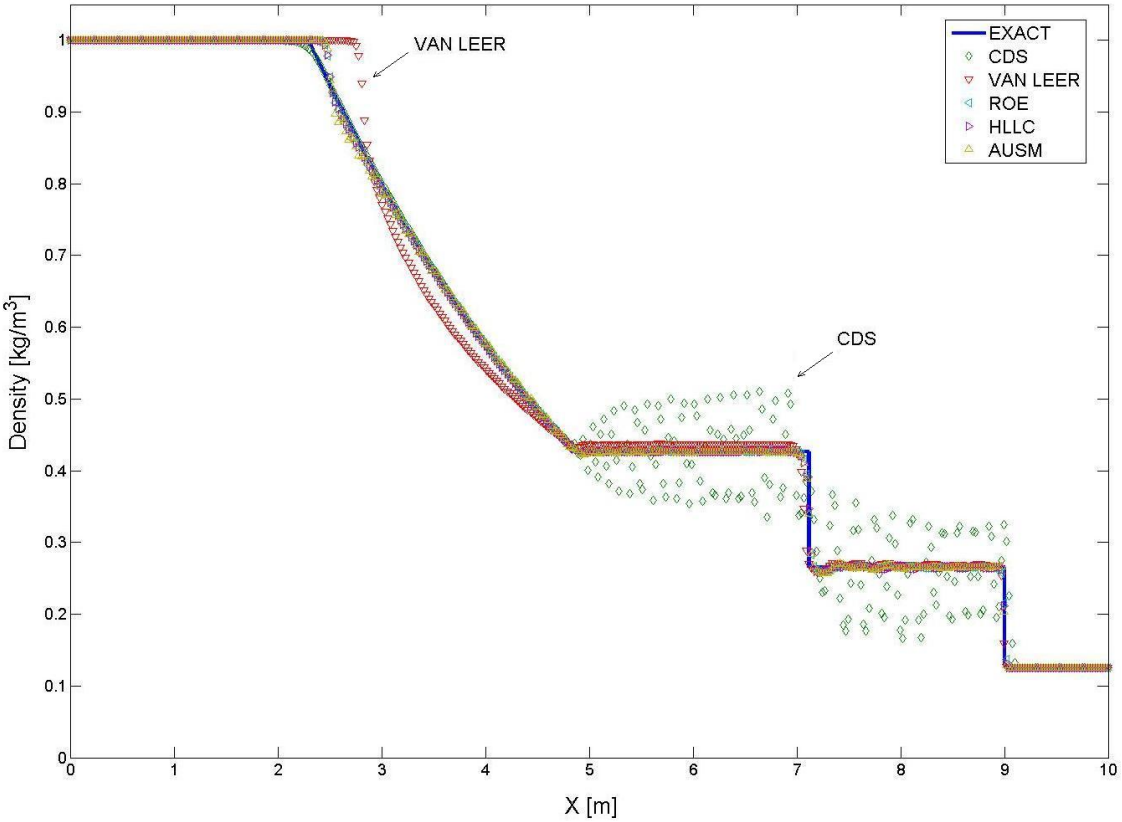

Figure 2. Shock tube flow with moderate pressure ratio (van Albada limiter).

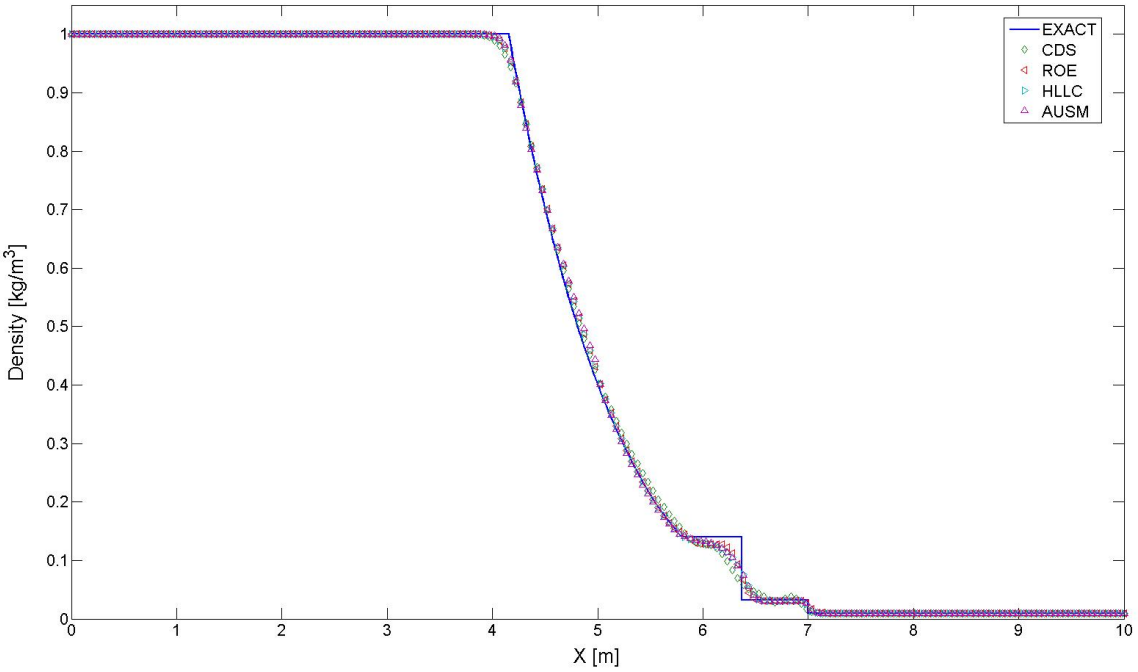

Figure 3. Shock tube flow with severe pressure ratio. van Albada limiter.

5.3 TEST CASE 3

According to Batten , the estimates of the signal velocities are not critical in situations which involve only weak wave interaction [Batten, 1997]. However, differences do arise in more demanding situations. A rather severe example would

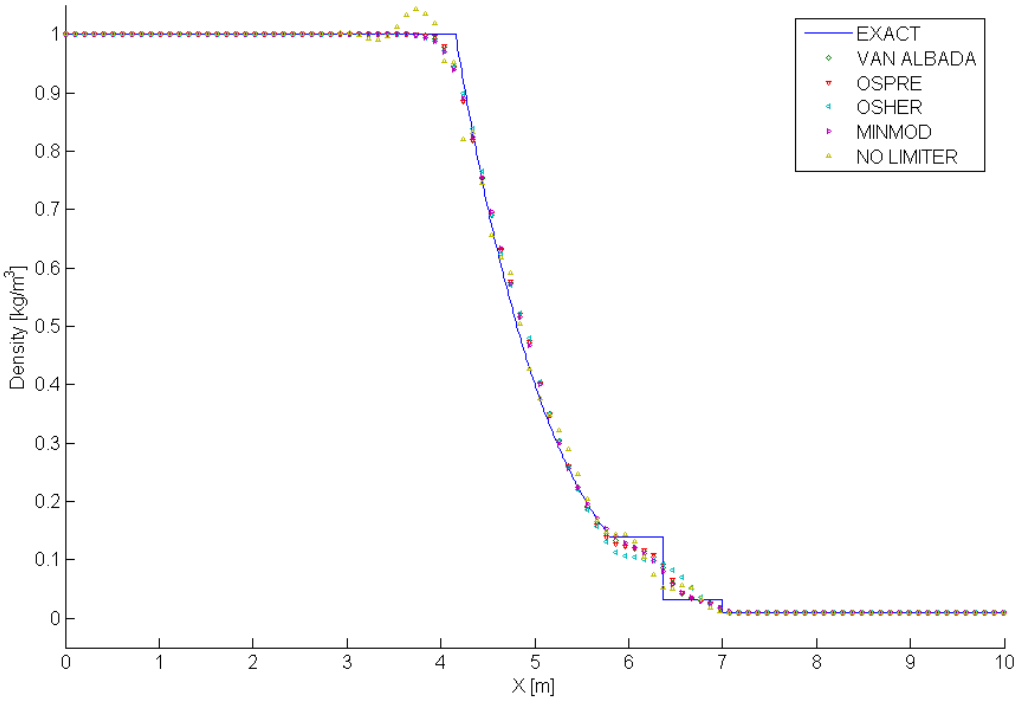

Figure 4. Shock tube flow with severe pressure ratio. HLLC flux scheme.

be the following compression shock-tube problem:

$$rho_L = rho_R = 1; \quad p_L = p_R = 1/\gamma; \quad u_L = 25; \quad u_R = -25$$

where the left ($x = -0.5$) and right ($x = 0.5$) ends of the shock-tube correspond to solid walls. Figure 5 shows results for this case at $t = 0.01$, computed using first-order scheme with 400 grid points. The bursting membrane causes two identical gases to move towards each other at Mach 25, while the inward moving rarefaction waves leave, theoretically, vacuum conditions near the two ends of the tube.

The Roe's scheme and Van Leert's scheme fail in the first few time steps and AUSM scheme gave a misleading solution. HLLC was able to resolve the severe transients of test case 3, eventhough there may be some questions regarding the application of the Euler equations to a flow where the continuum assumption no longer applies. Although most applications of engineering interest are not so severe, vacuum or near-vacuum conditions can often occur in initial transients. Furthermore, linearised approximate Riemann solvers are known to fail with negative pressures well before the vacuum state is reached [Batten, 1997].

6. CONCLUDING REMARKS

The main objective of the present research work consists of studying flux schemes to solve shock wave discontinuities. The flux schemes that are most used to capture shock waves have been tested and compared to analytical solutions. As expected, the Centred Jameson presented non-physical oscillations and attained convergence with rather low CFL. The Van Leer scheme presented dissipative behaviour resolving expansion fan. Roe and AUSM scheme resolved test cases 1 and 2 accordingly but were unable to resolve test case 3. HLLC attained good results for all test cases.

Various limiters were tested. All limiter options attained quite similar results preventing non-physical oscillations on discontinuities. Osher limiter, however, presented perceptible oscillation in the expansion wave. In any case, the need for limiting nearby discontinuities is clear from the results without a limiter operation.

All methods presented shock wave smearing. The smearing is minimized only through mesh refinement and lower CFL and thus increasing processing time significantly. Nonetheless, acoustic and entropy wave speeds were well estimated.

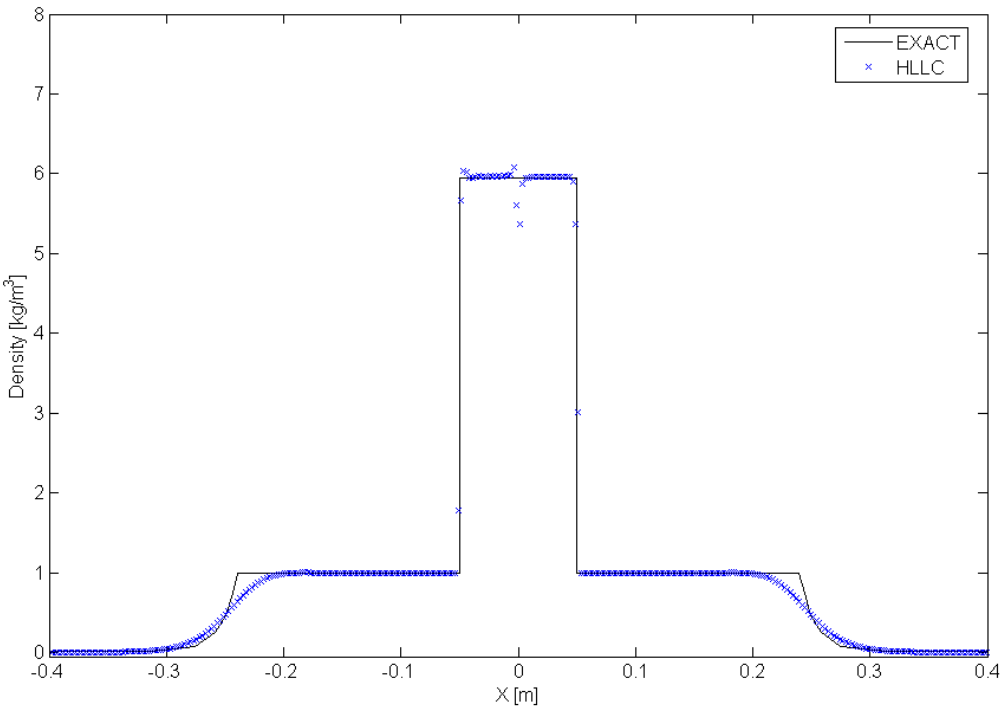

Figure 5. Compression shock tube flow. 1st order.

7. REFERENCES

Aliabadi, S., Tu, S., 2005, "A Slope Limiting Procedure in Discontinuous Galerkin Finite Element Method for Gasdynamics Applications", International Journal of Numerical Analysis and Modeling, Vol. 2, Number 2, Pages 163-178.

Batten, P., et al.,1997, "Average-State Jacobians and Implicit Methods for Compressible Viscous and Turbulent Flows". Journal of Computational Physics. Vol 137. Pages 38-78.

Bigarella, Enda, 2007, "Advanced Turbulence Modelling For Complex Aerospace Applications", Thesis - Instituto Tecnológico Aeronáutica, São José dos Campos

Davis, S. F., 1988, "Simplified Second-Order Godunov-type Methods", SIAM J. Sci. Statist. Comput., 9, 445-473.

S. K. Godunov. A Difference Method for the Numerical Calculation of Discontinuous Solutions of Hydrodynamic Equations. Mat. Sb. 47, 271, (1959).

Harten,A., Lax,P. and van Leer, B., 1983,"On Upstream Diőerencing and Godunov-type Schemes for Hyperbolic Conservation Laws," SIAM Rev., 25, 35-61.

Hirsch, C., 1990, Numerical Computation of Internal and External Flows, vol 2, Wiley.

Jameson, A.; Schmidt, W., Turkel, E.,"Numerical solution of the euler equations by finite volume methods using runge-kutta time-stepping schemes. In: 14th AIAA Fluid and Plasma Dynamics Conference. Palo Alto, CA: [s.n., 1981. (AIAA Paper No. 81-1259).

Harten,A., "High Resolution Schemes for Hyperbolic Conservation Laws", Journal of Computation Physics, Vol 49. Pages 357-385, 1983.

Laney, Culbert, Computational Gas Dynamics, Cambridge, UK: Cambridge University Press, 1998.

Leveque, R. J., 2002, "Finite Volume Methods for Hyperbolic Problems, Cambridge University Press".

Liou, Meng-Sing and Steffen, Christopher, J. Jr.,1993, "A New Flux Splitting Scheme". Journal of Computational Physics. Vol 107. Pages 23-39.

MacLean,M.,"Gryphon Euler Quasi One-Dimensional Euler Solver",Euler 1-D Compressible Flow Page,4 Feb. 2008 <http://chimeracfd.com/programming/gryphon/index.html>.

Roe, P. L."The Use of the Riemann Problem in Finite Difference Schemes". Lecture Notes in Physics. Vol 141. New York: Springer-Verlag. Pages 354-359. 1980

P. L. Roe, "Approximate Riemann Solvers, Parameter Vectors and Difference Schemes", Journal of Computational Physics

Vol. 43, 357, (1981).
B. Einfeldt, C. D. Munz, P. L. Roe, and B. Sjogreen., "On Godunov-Type Methods Near Low Densities". J. Comput. Phys. 92, 273 (1991).
Sod, G. A. (1978), "A Numerical Study of a Converging Cylindrical Shock.", J. Fluid Mechanics, 83, 785Ű794.
Toro,E. F., "Riemann Solvers and Numerical Methods for Fluid Dynamics," Springer, New York, 1999.
Van Leer,B., "Lecture Notes in Physics 170 (Springer-Verlag, New York/Berlin 1982), p.507.

8. Responsibility notice

The author(s) is (are) the only responsible for the printed material included in this paper